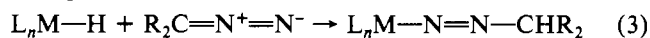
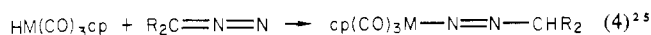


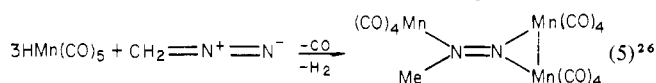
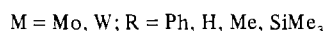
moiety to the C=N=N unit of the diazoalkane molecule, so as to generate an alkyldiazenido complex. This result can be exemplified as



Herrmann reported the most significant examples of such a reaction:

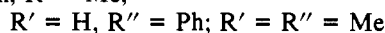
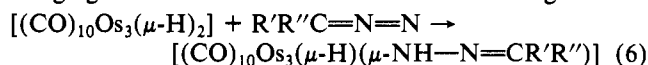


VI



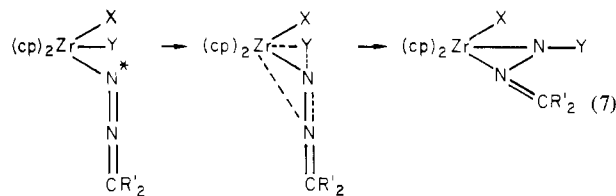
VII

Unlike reactions 4 and 5, reactions 1 and 2 formally represent the addition of the Zr-H and Zr-C fragments to the N=N= unit of a diazoalkane molecule. They exemplify the formation of a nitrogen-carbon and a nitrogen-hydrogen bond by the insertion of molecules resembling dinitrogen into metal-carbon and metal-hydrogen bonds. A very recent report^{2b} describes the reaction of diazoalkanes with an Os-H unit in [(CO)₁₀Os₃(μ-H)₂], affording an η¹-hydrazonato(1-) ligand bridging two metal atoms with the terminal nitrogen:

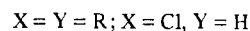


- (25) Herrmann, W. A.; Biersack, H. *Chem. Ber.* 1977, 110, 896-915. Herrmann, W. A. *Angew. Chem., Int. Ed. Engl.* 1975, 14, 355-6. Hillhouse, G. L.; Haymore, B. L.; Herrmann, W. A. *Inorg. Chem.* 1979, 18, 2423-6. Lappert, M. F.; Poland, J. S. *J. Chem. Soc., Chem. Commun.* 1969, 1061-2.
- (26) Herrmann, W. A.; Ziegler, M. L.; Weidenhammer, K. *Angew. Chem., Int. Ed. Engl.* 1976, 15, 368-9. Herrmann, W. A.; Biersack, H.; Mayer, K. K.; Reiter, B. *Chem. Ber.* 1980, 113, 2655-65.

Diazoalkane can be considered as having its N-N unit highly polarized by an electron-rich center (the carbene moiety). Moreover, we can consider as a preliminary step in reactions 1 and 2, leading to the insertion of a diazoalkane molecule, the coordination of the diazoalkane molecule on the acidic zirconium center, as sketched in VIII. VIII may be



VIII



considered a plausible intermediate preceding the migration of the alkyl or hydrido group to the diazoalkane. The incoming ligand may labilize the M-C and M-H bonds, providing in close proximity an insertable group for the migrating ligand. The η² bonding mode is the consequence of the changed geometry around N*, when the Y group migrates to it in a concerted type process.

Acknowledgment. This work was supported by the CNR (Rome).

Registry No. I, 85650-33-5; II, 82942-37-8; III, 85650-32-4; IV, 37342-97-5; V, 82942-38-9; Cp₂ZrMe₂, 12636-72-5; Cp₂Zr(CH₂Ph)₂, 37206-41-0; Ph₂C=N=N, 883-40-9; (EtOCO)₂C=N=N, 5256-74-6.

Supplementary Material Available: Listings of observed and calculated structure factors, coordinates for hydrogen atoms (Tables SI-SIII), thermal parameters (Tables SIV-SVI), bond distances and angles (Table SVII), and equations of least-squares planes (Table SVIII) (50 pages). Ordering information is given on any current masthead page.

Contribution from the Department of Chemistry, University of Minnesota, Minneapolis, Minnesota 55455

Nucleophilic Nitrosylations of Metal Carbonyls Using Bis(triphenylphosphine)nitrogen(1+) Nitrite

ROBERT E. STEVENS and WAYNE L. GLADFELTER*

Received October 18, 1982

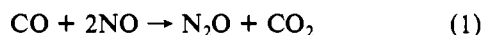
Bis(triphenylphosphine)nitrogen(1+) nitrite (PPN(NO₂)) has been found to be very effective for converting metal carbonyls into nitrosyl carbonyl complexes. The reactions are conducted in dipolar aprotic solvents such as tetrahydrofuran (THF) or acetonitrile and characteristically give high yields with no side products. The reaction has been successfully applied to Fe(CO)₅, [Mn(CO)₆]⁺, [Mn(CO)₅(CH₃CN)]⁺, [Fe(CO)₂(PPh₃)₂(NO)]⁺, Mn(CO)₄(NO), Mn₂(CO)₁₀, Co₂(CO)₈, Fe₃(CO)₁₂, Ru₃(CO)₁₂, Os₃(CO)₁₂, and Ru₆C(CO)₁₇ to generate CO₂, a two-electron donor ligand (L), and the product, resulting in replacement of CO and L with NO and a negative charge. A kinetic analysis of the reaction of Fe(CO)₅ and PPN(NO₂) in acetonitrile verifies that the reaction is first order in iron and nitrite with $k = 0.111 \pm 0.007 \text{ M}^{-1} \text{ s}^{-1}$ at $26 \pm 1^\circ \text{C}$. The addition of a 10-fold excess of PPh₃ had no effect on the rate of the reaction. The new nitrosylcarbonylmetalate, [Mn(CO)₂(NO)₂]⁻, was characterized by a single-crystal X-ray crystallographic study (*P*₂₁/*a* space group, *Z* = 4, *a* = 21.890 (5) Å, *b* = 9.194 (3) Å, *c* = 17.495 (3) Å, β = 96.25 (2)°), which shows that it has a tetrahedral geometry with disordered NO and CO ligands. Characterization of the new clusters [Ru₃(CO)₁₀(NO)]⁻ and [Os₃(CO)₁₀(NO)]⁻ establishes that the NO is bridging one edge of the metal triangle, while spectroscopic evidence suggests that [Ru₆C(CO)₁₅(NO)]⁻ contains a terminal nitrosyl ligand. Nitrogen-15 magnetic resonance spectra of the bridging nitrosyls exhibit a 400 ppm downfield shift relative to the resonance of mononuclear nitrosyl carbonyl compounds. In some cases PPN(NO₂) simply substitutes a NO₂⁻ for a carbonyl. This occurs with Co(CO)₃(NO) to give the new nitro nitrosyl product [Co(NO₂)(C-O)₂(NO)]⁻.

Introduction

Unlike carbon monoxide, nitric oxide is not one of the basic building blocks of the chemical industry. If anything, there has been much work devoted to develop efficient means to

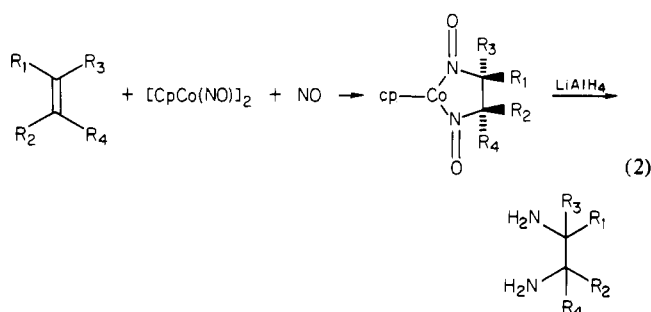
destroy NO. With this in mind, it is worth mentioning some of the reasons for the interest in the nitrosyl ligand. We can designate two categories of reactivity of metal nitrosyl complexes: those reactions directly involving the NO ligand and

those in which NO is an ancillary ligand. Equation 1 shows



the reaction in which NO is reduced to the less toxic molecule N₂O. This reaction, which is important for the control of NO in exhausts, is catalyzed by heterogeneous and homogeneous systems. In both cases, metal nitrosyls are important intermediates.^{1,2}

A relatively new catalytic process that directly involves the M-NO group is the oxidation of olefins or alcohols with molecular oxygen.³⁻⁶ This employs the metal nitro to metal nitrosyl conversion and subsequent reaction of the bent NO with O₂ to regenerate the starting nitro complex. Stoichiometric reactions of coordinated nitric oxide are more common yet often complex and poorly understood.² The nitroprusside ion has long been used as a reagent in qualitative analysis because of the colors produced when it reacts with nucleophiles.⁷ The site of attack on [Fe(CN)₅(NO)]²⁻ is at the NO ligand. For instance, with OH⁻, [Fe(CN)₅(NO₂)]⁴⁻ is produced,⁸ while with compounds having enolizable hydrogens such as acetone, the oxime species CH₃-C(O)-CH(NO₂) is isolated.⁹ This reactivity is also interesting because it involves the formation of a C-N bond. A different approach to the formation of C-N bonds has recently led to a new method of 1,2-diamination of alkenes¹⁰ (eq 2). The intermediate in this reaction is believed to be the dinitrosyl cpCo(NO)₂.

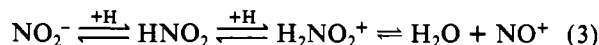


As a common ancillary ligand, NO, which is considered to be the most effective π -accepting ligand, plays an important role as an activating group. Much work has centered around the linear-to-bent conversion of the M-NO group, which formally results in an unsaturated metal complex.¹¹ Many substitution reactions of carbonyl nitrosyl complexes involve such intermediates,¹² and the extension of this conversion in mononuclear complexes to homogeneous catalytic reactions has been explored. One example of a catalytic reaction involving a nitrosyl complex is the dimerization of dienes using Fe(NO)₂(THF)_n,¹³ although it is unclear that the linear-to-bent conversion is involved in the mechanism. A method utilizing NO to activate molecules toward nucleophiles involves the isoelectronic nature of CO and NO⁺. For instance, cpRe(CO)₃ is not a very effective electrophile; however, sub-

stitution of a CO with NO⁺ gives [cpRe(CO)₂(NO)]⁺, which is very susceptible to nucleophilic attack at the coordinated carbonyls.¹⁴⁻¹⁷ One of the more remarkable examples of this activating effect involves [cpMo(allyl)(CO)(NO)]⁺, which reacts with nucleophiles at the terminus of the allyl ligand. Here NO⁺ not only activates the molecule toward nucleophilic attack, but the difference between NO and CO directs the stereochemistry of this reaction.¹⁸

Although few studies exist on the chemistry of the NO ligand on metal clusters, we have recently reported¹⁹ that coordinated NO can be readily deoxygenated, generating nitrido clusters and CO₂. This reaction is interesting because it involves the oxidative removal of one CO of the cluster to generate a vacant site.²⁰ We have also observed the first well-defined examples of O-methylation and O-protonation of a metal nitrosyl.²¹

The synthesis of metal nitrosyls has been problematic.²² Many of the reagents themselves such as NO gas and NO⁺ are so reactive that undesired side reactions commonly occur. Since we are particularly interested in exploring the chemistry of nitrosyl carbonyl clusters, we had to develop improved methods for introducing the NO ligand into a complex. Nitrite has been used to prepare metal nitrosyls in two distinctly different modes. By far, the more common technique has involved the reaction of nitrite in acidic media, which is simply a source (usually less expensive) of the nitrosonium ion via eq 3. The second technique, which was first applied to metal



carbonyls by Hieber and Beutner,²³ makes use of nitrite in basic media. Equation 4 shows the prototypal reaction with Fe(CO)₅ + NaNO₂ + NaOCH₃ →



Fe(CO)₅. Although this reaction was first reported in 1963, a direct extension of it to other metal carbonyls has not been reported to give the products analogous to [Fe(CO)₃(NO)]⁻. For instance, the reaction of nitrite and methoxide with Mo(CO)₆ resulted in the formation of two unusual clusters that, although they did contain a nitrosyl ligand on each Mo, also incorporated methoxide into their frameworks.²⁴ All of these reactions were conducted in protic solvents, usually alcohols. We entertained the idea that leaving protic media would have two beneficial effects. First, product stability would likely be enhanced. These reactions result in a substantial increase in negative charge being located at the metal. Particularly with the anionic products, an acid-base equilibrium could exist, which would generate the metal hydride. Such species are often unstable; for example, HFe(CO)₃(NO) decomposes rapidly above -45 °C.²³ This type of acid-base equilibrium would be expected to become increasingly important in moving to the left and down the periodic table from iron. The second benefit of leaving protic solvents would be to increase the nucleophilicity of NO₂⁻. The immediate problem in leaving protic solvents is the insolubility of NaNO₂ in many of the

- (1) Eisenberg, R.; Hendriksen, D. E. *Adv. Catal.* **1979**, *28*, 79.
- (2) McCleverty, J. A. *Chem. Rev.* **1979**, *79*, 53.
- (3) Tovrog, B. S.; Mares, F.; Diamond, S. E. *J. Am. Chem. Soc.* **1980**, *102*, 6616.
- (4) Andrews, M. A.; Kelly, K. P. *J. Am. Chem. Soc.* **1981**, *103*, 2894.
- (5) Tovrog, B. S.; Diamond, S. E.; Mares, F.; Szalkiewicz, A. *J. Am. Chem. Soc.* **1981**, *103*, 3522.
- (6) Andrews, M. A.; Cheng, C.-W. F. *J. Am. Chem. Soc.* **1982**, *104*, 4268.
- (7) Swinehart, J. H. *Coord. Chem. Rev.* **1967**, *2*, 385.
- (8) Swinehart, J. H.; Rock, P. A. *Inorg. Chem.* **1966**, *5*, 573.
- (9) Swinehart, J. H.; Schmidt, W. G. *Inorg. Chem.* **1967**, *6*, 232.
- (10) Becker, P. N.; White, M. A.; Bergman, R. G. *J. Am. Chem. Soc.* **1980**, *102*, 5676.
- (11) Dolcetti, G.; Hoffman, N. W.; Collman, J. P. *Inorg. Chim. Acta* **1972**, *6*, 531.
- (12) Morris, D. E.; Basolo, F. *J. Am. Chem. Soc.* **1968**, *90*, 2531.
- (13) Ballivet-Tkatchenko, D.; Riveccie, M.; El Murr, N. *J. Am. Chem. Soc.* **1979**, *101*, 2763.

- (14) Nesmeyanov, A. N.; Anisimov, K. N.; Kolobova, N. E.; Krasnoslobodskaya, L. L. *Izv. Akad. Nauk SSSR, Ser. Khim.* **1970**, 860.
- (15) Tam, W.; Wong, W.; Gladysz, J. A. *J. Am. Chem. Soc.* **1979**, *101*, 1589.
- (16) Sweet, J. R.; Graham, W. A. G. *J. Am. Chem. Soc.* **1982**, *104*, 2811.
- (17) Casey, C. P.; Andrews, M. A.; McAlister, D. R.; Rinz, J. E. *J. Am. Chem. Soc.* **1980**, *102*, 1927.
- (18) Adams, R. D.; Chodosh, D. F.; Faller, J. W.; Rosan, A. M. *J. Am. Chem. Soc.* **1979**, *101*, 2570.
- (19) Fjare, D. E.; Gladfelter, W. L. *Inorg. Chem.* **1981**, *20*, 3533.
- (20) Fjare, D. E.; Gladfelter, W. L., to be submitted for publication.
- (21) Stevens, R. E.; Gladfelter, W. L. *J. Am. Chem. Soc.* **1982**, *104*, 6454.
- (22) Caulton, K. G. *Coord. Chem. Rev.* **1975**, *14*, 317.
- (23) Hieber, W.; Beutner, H. Z. *Anorg. Allg. Chem.* **1963**, *320*, 101.
- (24) Kirtley, S. W.; Chanton, J. P.; Love, R. A.; Tipton, D. L.; Sorrell, T. N.; Bau, R. *J. Am. Chem. Soc.* **1980**, *102*, 3451.

common aprotic solvents. We found²⁵ and discuss here that the bis(triphenylphosphine)nitrogen(1+) salt allows us to use NO_2^- in solvents such as THF and CH_3CN to improve the syntheses of several known compounds and prepare several new nitrosyl carbonyl complexes.

Experimental Section

$\text{PPN}(\text{Cl})$,²⁶ $\text{PPN}(\text{NO}_2)$,²⁷ $\text{Ru}_3(\text{CO})_{12}$,²⁸ $[\text{Mn}(\text{CO})_5]\text{BF}_4$,²⁹ $[\text{Mn}(\text{CO})_5(\text{CH}_3\text{CN})]\text{PF}_6$,³⁰ $\text{Co}(\text{CO})_3(\text{NO})$,³¹ $[\text{Fe}(\text{CO})_2(\text{PPh}_3)_2(\text{NO})]\text{PF}_6$,³² and $\text{Ru}_6\text{C}(\text{CO})_{17}$ ³³ were prepared according to published procedures. $\text{Fe}(\text{CO})_5$, $\text{Co}_2(\text{CO})_8$, $\text{Mn}_2(\text{CO})_{10}$, and $\text{Os}_3(\text{CO})_{12}$ were purchased from Strem Chemical Co. Tetrahydrofuran (THF) and diethyl ether were dried by distillation from sodium benzophenone ketyl under N_2 . Acetonitrile, chloroform, and methylene chloride were dried by distillation from P_2O_5 under N_2 . Hexane was dried by distillation from CaH_2 under N_2 . All reactions were conducted under a N_2 atmosphere, which was maintained either up to the point of the first hexane extraction following acidification in the preparation of neutral compounds or until complete formation of crystals of the salts. Chromatography was conducted on silica gel. Infrared spectra were obtained on a Beckman 4240 spectrophotometer, and the NMR data were obtained on a Nicolet NTCFT-1180 300 MHz spectrophotometer. The samples for the ^{15}N NMR experiments were prepared from $\text{Na}^{15}\text{NO}_2$ (90% enriched) obtained from Merck Sharp and Dohme. Each ^{15}N NMR spectrum was conducted with CH_2Cl_2 as a solvent (~ 3.5 mL) in a 12-mm tube with a sample concentration approximately 0.03 M and $\text{Cr}(\text{acac})_3$ (53 mg) added. The referencing was done externally with use of CH_3NO_2 in CHCl_3 with 0.03 M $\text{Cr}(\text{acac})_3$ set at 379.60 ppm downfield from NH_3 (liquid, 25 °C).³⁴ All data are reported relative to NH_3 . With an acquisition time of 2.63 s, excellent signal-to-noise ratio was obtained with ~ 500 scans.

Preparation of $\text{PPN}[\text{Fe}(\text{CO})_3(\text{NO})]$. $\text{PPN}(\text{NO}_2)$ (503.4 mg, 0.861 mmol) was placed in a Schlenk tube, and THF (60 mL) was added via syringe. Very little of the white solid dissolved until $\text{Fe}(\text{CO})_5$ (0.116 mL, 0.863 mmol) was added via syringe. Immediate effervescence was observed, and the solution turned yellow as the $\text{PPN}(\text{NO}_2)$ reacted. After 30 min, the reaction was complete; all of the solid had dissolved, and a clear yellow solution remained. The solvent was removed on a rotary evaporator, giving bright yellow crystals of $\text{PPN}[\text{Fe}(\text{C}(\text{O})_3(\text{NO}))]$. The crude product was recrystallized from methylene chloride/diethyl ether to give an 87% yield of purified air-stable $\text{PPN}[\text{Fe}(\text{CO})_3(\text{NO})]$ (527.3 mg, 0.774 mmol). Anal. Calcd for $\text{FeP}_2\text{O}_4\text{N}_2\text{C}_{39}\text{H}_{30}$: C, 66.12; H, 4.43; N, 3.95. Found: C, 66.42; H, 4.43; N, 4.08.

Preparation of $\text{PPN}(\text{NO}_2)$. $\text{PPN}(\text{Cl})$ (860.9 mg, 1.50 mmol) was dissolved in 18 mL of hot distilled water (~ 60 °C). $\text{Na}^{15}\text{NO}_2$ (105.0 mg, 1.50 mmol) was dissolved in 1 mL of distilled water at room temperature. The $\text{PPN}(\text{Cl})$ solution was added dropwise to the $\text{Na}^{15}\text{NO}_2$ solution with stirring. A white precipitate was observed. The mixture was cooled with stirring to 0 °C with an ice bath and filtered. The white microcrystalline product was washed with 2×10 mL of cold distilled water and 3×10 mL of diethyl ether. The resulting product was air-dried overnight to give $\text{PPN}(\text{NO}_2) \cdot \text{H}_2\text{O}$ (876.2 mg, 1.45 mmol). The water of crystallization was removed via an azeotropic distillation with benzene to give anhydrous $\text{PPN}(\text{NO}_2)$ (833.4 mg, 1.42 mmol) in 95% yield.

Preparation of $\text{PPN}[\text{Mn}(\text{CO})_2(\text{NO})_2]$. To a stirred solution of $[\text{Mn}(\text{CO})_5(\text{CH}_3\text{CN})]\text{PF}_6$ (209.3 mg, 0.549 mmol) in CH_3CN (6 mL) was added dropwise a solution of $\text{PPN}(\text{NO}_2)$ (283.0 mg, 0.484 mmol) in CH_3CN (10 mL) over a period of 25 min. During the addition the solution changed from a cloudy white to a clear deep red-orange. The resulting solution, containing principally $\text{Mn}(\text{CO})_4(\text{NO})$ with a minor component of $[\text{Mn}(\text{CO})_2(\text{NO})_2]^-$, was distilled under partial

vacuum into a flask containing $\text{PPN}(\text{NO}_2)$ (280.3 mg, 0.480 mmol). The $\text{Mn}(\text{CO})_4(\text{NO})$ distilled with the solvent, leaving some $\text{PPN}[\text{Mn}(\text{CO})_2(\text{NO})_2]$ and $\text{PPN}(\text{PF}_6)$ in the original reaction vessel. The solution of $\text{Mn}(\text{CO})_4(\text{NO})$ and $\text{PPN}(\text{NO}_2)$ in acetonitrile was stirred at room temperature for 1.5 h. The solvent was then removed to give crude red-orange crystalline product. The product was recrystallized from THF/diethyl ether to give slightly air-sensitive red-orange microcrystals of $\text{PPN}[\text{Mn}(\text{CO})_2(\text{NO})_2]$ (245.4 mg, 0.346 mmol) in 72% yield. Anal. Calcd for $\text{MnP}_2\text{O}_4\text{N}_3\text{C}_{38}\text{H}_{30}$: C, 64.32; H, 4.26; N, 5.92. Found: C, 64.54; H, 4.46; N, 5.79.

Preparation of $\text{Fe}(\text{CO})(\text{PPh}_3)(\text{NO})_2$. $[\text{Fe}(\text{CO})_2(\text{PPh}_3)_2(\text{NO})]\text{PF}_6$ (208.0 mg, 0.256 mmol) and $\text{PPN}(\text{NO}_2)$ (230.0 mg, 0.393 mmol) were degassed, and CH_3CN (8 mL) was added via syringe. The reaction was stirred for 30 min, and the solvent was then removed under vacuum. The residue was extracted with a 4:1 hexane/ CH_2Cl_2 mixture and chromatographed. The solvent from the resulting red band was evaporated to dryness, giving red crystals of $\text{Fe}(\text{CO})(\text{PPh}_3)(\text{NO})_2$ (56.0 mg, 0.128 mmol) in 50% yield. The product was identified by its infrared spectrum.³⁵

Preparation of $\text{PPN}[\text{Co}(\text{NO}_2)(\text{CO})_2(\text{NO})]$. $\text{PPN}(\text{NO}_2)$ (115.5 mg, 0.197 mmol) was placed in a Schlenk tube, and THF (15 mL) was added via syringe. Very little of the white solid dissolved until $\text{Co}(\text{CO})_3(\text{NO})$ (0.20 mL, 1.70 mmol) was added via syringe. Immediate gas evolution was observed, and the solution turned deep red-orange as the $\text{PPN}(\text{NO}_2)$ reacted. The reaction was allowed to stir 1 h, at which point all of the solid had reacted and a clear red-orange solution remained. The solvent and excess $\text{Co}(\text{CO})_3(\text{NO})$ were removed in vacuo, and the crude product was recrystallized from THF/diethyl ether to give a 64% yield of air-sensitive $\text{PPN}[\text{Co}(\text{NO}_2)(\text{CO})_2(\text{NO})]$ (94.1 mg, 0.129 mmol). Anal. Calcd for $\text{CoP}_2\text{O}_5\text{N}_3\text{C}_{38}\text{H}_{30}$: C, 62.56; H, 4.14; N, 5.76. Found: C, 62.64; H, 4.28; N, 5.66.

Reaction of $\text{PPN}(\text{NO}_2)$ with $\text{Co}_2(\text{CO})_8$. $\text{Co}_2(\text{CO})_8$ (180.0 mg, 0.526 mmol) and $\text{PPN}(\text{NO}_2)$ (270.0 mg, 0.462 mmol) were degassed, and THF (15 mL) was added via syringe. Gas evolution was observed, and the solution turned red-orange. Infrared spectroscopy showed the presence of only $\text{Co}_2(\text{CO})_8$, $[\text{Co}(\text{CO})_4]^-$, and $\text{Co}(\text{CO})_3(\text{NO})$.

Reaction of $\text{PPN}(\text{NO}_2)$ with $\text{Mn}_2(\text{CO})_{10}$. $\text{Mn}_2(\text{CO})_{10}$ (56.0 mg, 0.144 mmol) was dissolved in THF (15 mL) to give a yellow solution. $\text{PPN}(\text{NO}_2)$ (79.0 mg, 0.135 mmol) was added as a solid to the yellow solution. The solution slowly turned orange over a period of 20 min, and some $\text{PPN}(\text{NO}_2)$ was still undissolved. An infrared spectrum of the orange solution showed the presence of only $\text{Mn}_2(\text{CO})_{10}$, $[\text{Mn}(\text{CO})_5]^-$, and $[\text{Mn}(\text{CO})_2(\text{NO})_2]^-$. No $\text{Mn}(\text{CO})_4(\text{NO})$ was observed.

Preparation of $\text{PPN}[\text{Ru}_3(\text{CO})_{10}(\text{NO})]$. $\text{Ru}_3(\text{CO})_{12}$ (251.8 mg, 0.395 mmol) and $\text{PPN}(\text{NO}_2)$ (254.2 mg, 0.435 mmol) were degassed, and freshly distilled THF (40 mL) was added via syringe. Gas evolution was observed as the solution became deep yellow-red. The reaction was stirred for 30 min at which point no solids were observed. The volume of the solution was reduced under vacuum to 8 mL, and 40 mL of diethyl ether was added via syringe, forming a cream-colored precipitate and a deep yellow solution. The solution was filtered, and the residue was washed with 10 mL of diethyl ether. The product was precipitated with hexane to give green, slightly air-sensitive microcrystals of $\text{PPN}[\text{Ru}_3(\text{CO})_{10}(\text{NO})]$ in 93% yield (420.9 mg, 0.365 mmol). Anal. Calcd for $\text{Ru}_3\text{P}_2\text{O}_{11}\text{N}_2\text{C}_{46}\text{H}_{30}$: C, 47.96; H, 2.62; N, 2.43. Found: C, 47.73; H, 2.80; N, 2.38.

Preparation of $\text{PPN}[\text{Os}_3(\text{CO})_{10}(\text{NO})]$. This salt was prepared from $\text{Os}_3(\text{CO})_{12}$ and $\text{PPN}(\text{NO}_2)$ by using the same procedure as for the ruthenium analogue. Slightly air-sensitive yellow-green microcrystals of $\text{PPN}[\text{Os}_3(\text{CO})_{10}(\text{NO})]$ were obtained in 88% yield. Anal. Calcd for $\text{Os}_3\text{P}_2\text{O}_{11}\text{N}_2\text{C}_{46}\text{H}_{30}$: C, 38.93; H, 2.13; N, 1.97. Found: C, 38.74; H, 2.17; N, 1.88.

Protonation of $\text{PPN}[\text{Ru}_3(\text{CO})_{10}(\text{NO})]$. At room temperature $\text{CF}_3\text{CO}_2\text{H}$ (9.0 μL , 0.117 mmol) was added to $\text{PPN}[\text{Ru}_3(\text{CO})_{10}(\text{NO})]$ (108.1 mg, 0.094 mmol) in CH_2Cl_2 (20 mL). The solvent was removed under vacuum, and the residue was extracted into hexane. Chromatography of the yellow hexane extract gave only one band. Evaporation of the hexane gave 31.9 mg (55% yield) of deep yellow crystalline product. An infrared spectrum of the product confirmed its identity as $\text{HRu}_3(\text{CO})_{10}(\text{NO})$.³⁶

(25) Stevens, R. E.; Yanta, T. J.; Gladfelter, W. L. *J. Am. Chem. Soc.* **1981**, *103*, 4981.

(26) Ruff, J. K.; Schlientz, W. J. *Inorg. Synth.* **1974**, *15*, 84.

(27) Martinsen, A.; Songstad, J. *Acta Chem. Scand., Ser. A* **1977**, *A31*, 645.

(28) Mantovani, A.; Cenini, S. *Inorg. Synth.* **1976**, *16*, 47.

(29) Beach, N. A.; Gray, H. B. *J. Am. Chem. Soc.* **1968**, *90*, 5713.

(30) Drew, D.; Darensbourg, D. J.; Darensbourg, M. Y. *Inorg. Chem.* **1975**, *14*, 1579.

(31) Job, R.; Rovang, J. *Synth. React. Inorg. Met.-Org. Chem.* **1976**, *6*, 367.

(32) Johnson, B. F. G.; Segal, J. A. *J. Chem. Soc., Dalton Trans.* **1972**, 1268.

(33) Johnson, B. F. G.; Lewis, J.; Williams, I. G. *J. Chem. Soc. A* **1970**, 901.

(34) Levy, G. C.; Lichter, R. L. "Nitrogen-15 Nuclear Magnetic Resonance Spectroscopy"; Wiley: New York, 1979.

(35) McBride, D. W.; Stafford, S. L.; Stone, F. G. A. *Inorg. Chem.* **1962**, *1*, 386.

(36) Johnson, B. F. G.; Raithby, P. R.; Zuccaro, C. *J. Chem. Soc., Dalton Trans.* **1980**, 99.

Table I

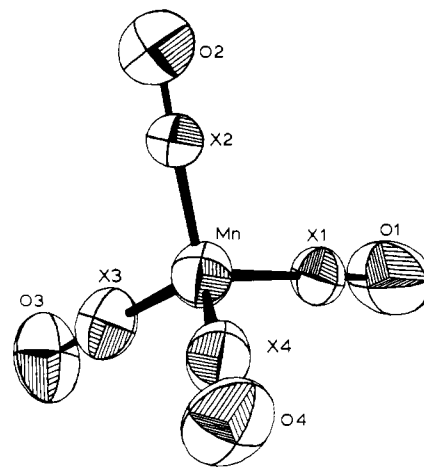
Crystal Parameters	
cryst system: monoclinic	$V = 3500 (3) \text{ \AA}^3$
space group: $P2_1/a$	$Z = 4$
$a = 21.890 (5) \text{ \AA}$	calcd density = 1.35 g cm^{-3}
$b = 9.194 (3) \text{ \AA}$	temp = 22°C
$c = 17.495 (3) \text{ \AA}$	abs coeff = 5.34 cm^{-1}
$\beta = 96.25 (2)^\circ$	formula: $\text{MnP}_2\text{O}_4\text{N}_3\text{C}_{38}\text{H}_{30}$

Measurement Intensity Data	
diffractometer: Enraf-Nonius CAD 4	
radiation: Mo $K\alpha$ ($\lambda = 0.71069 \text{ \AA}$)	
monochromator: graphite crystal	
scan speed: variable from 1.00 to $20.0^\circ/\text{min}$	
scan range: $0^\circ \leq 2\theta \leq 50^\circ$	
reflens measd: $\pm h, +k, +l$	
check reflens: $\{040\}$, $\{823\}$, $\{537\}$; measd approximately every 200 reflens	
reflens collected: 5628 unique reflens; 3061 with $I > 2\sigma(I)$	
$p = 0.05$	
$R = 0.063$	
$R_w = 0.081$	
error in observation of unit weight = 2.25	

Protonation of PPN[Os₃(CO)₁₀(NO)]. The protonation of PPN-[Os₃(CO)₁₀(NO)] with CF₃SO₃H was conducted analogously and gave HO₃(CO)₁₀(NO) as deep yellow crystals in 32% yield. The product was identified by its infrared spectrum.³⁶

Preparation of PPN[Ru₆C(CO)₁₅(NO)]. Ru₆C(CO)₁₇ (104 mg, 0.095 mmol) and PPN(NO₂) (56 mg, 0.096 mmol) were degassed, and freshly distilled THF (20 mL) was added via syringe. Gas evolution was observed as the solution turned clear deep red. The reaction was stirred for 20 min, at which point no solids were observed. The volume of the solution was reduced under vacuum to ~2 mL, and 40 mL of diethyl ether was added via syringe, forming an orange precipitate and a red-orange solution. The solution was filtered, and the residue was washed with 10 mL of diethyl ether. The product was precipitated with hexane to give red microcrystals of PPN-[Ru₆C(CO)₁₅(NO)] in 74% yield (113 mg, 0.074 mmol). Anal. Calcd for Ru₆P₂O₁₆N₂C₅₂H₃₀: C, 38.86; H, 1.88; N, 1.74. Found: C, 38.67; H, 2.03; N, 1.65.

Collection and Reduction of the X-ray Data. Red-orange crystals of PPN[Mn(CO)₂(NO)₂] were grown from a solution of THF/diethyl ether. A suitable crystal with approximate dimensions 0.2 × 0.1 × 0.08 mm was mounted on a glass fiber and sealed in a Lindemann capillary under N₂. The crystal was found to be primitive monoclinic by the Enraf-Nonius CAD 4-SDP peak search, centering, and indexing programs and by a Delauney reduction calculation.³⁷ Data collection was begun, and from the systematic absences ($0k0$, $k = 2n + 1$; $h0l$, $h = 2n + 1$) the unique space group $P2_1/a$ was unambiguously assigned. A summary of the crystal data is presented in Table I. Background counts were measured at both ends of the scan range with the use of an $\omega-2\theta$ scan, equal at each side to one-fourth of the scan range of the peak. In this manner, the total duration of measuring background is equal to half of the time required for the peak scan. Three reflections were monitored approximately every 200 reflections and showed no significant decay throughout the entire data collection. A total of 5628 unique reflections were measured, of which 3061 had $I > 2\sigma(I)$, and were used in the structural determination.³⁸ The data

Figure 1. View of [Mn(CO)₂(NO)₂]⁻ showing the atom labels.

were corrected for Lorentz, polarization, and background effects but not for absorption.

Solution and Refinement of the Structure. The structure was solved by conventional heavy-atom techniques. The position of the manganese atom was determined by a Patterson synthesis. Subsequent least-squares, Fourier, and difference Fourier calculations revealed the positions of the non-hydrogen atoms.³⁹ At this stage, as the atoms located around the manganese were found, they were all assigned as carbon atoms. All atoms in the anion and the P and N atoms of the cation were refined with the use of anisotropic temperature factors. After convergence was reached with all X atoms assigned as carbon, no compelling positions for the nitrogens were found. Our evaluation was based on the temperature factors and the Mn-X bond distances. At this point, positions X3 and X4 had slightly smaller temperature factors and nitrogens were assigned to these positions. Further refinement resulted in the nitrogen temperature factors increasing so that they were now larger than those for the carbons. The new Mn-N distances increased slightly, making the case for a fully ordered refinement unlikely. All X atoms were then considered fully disordered, and refinement was continued with each $X = \frac{1}{2}C + \frac{1}{2}N$. Once again, there were slight changes in Mn-X distances and the X temperature factors. It became apparent that with the current room-temperature data conclusive assignment of the nitrogen positions would not be possible. X-ray data collected at low temperature or preferably neutron data (where the C and N scattering factors differ by a greater amount) will be required to positively locate the C and N atoms in crystals of PPN[Mn(CO)₂(NO)₂]. After convergence with the disordered model, the hydrogen atom positions were calculated and used in the final cycles, but their positions and temperature factors [set by $B(H) = B(C) + 1.0$] were not refined or reset after each cycle. The final atom positions are listed in Table II. The values of the atomic scattering factors used in the calculations were taken from the usual tabulation, and the effects of anomalous dispersion were included for the non-hydrogen atoms.⁴⁰ The hydrogen atom scattering factors were taken from Cromer and Ibers' list.⁴¹

Fourier Transform Infrared Spectroscopy. Solutions of PPN(Cl), PPN[Ru₃(CO)₁₀(NO)], PPN[Os₃(CO)₁₀(NO)], PPN[Ru₃(CO)₁₀(¹⁵NO)], PPN[Co(NO₂)(CO)₂(NO)], and PPN[Co(¹⁵NO₂)(CO)₂(NO)] in chloroform were prepared with a standard concentration. The spectra were recorded on a Digilab FTIR/GCIR spectrophotometer or a Nicolet 7199 FTIR spectrophotometer in a 0.5-mm sealed NaCl cell. Subtraction of the absorptions due to the PPN⁺ cation resulted in the observation of $\nu(\text{NO})$ at 1479 and 1460 cm^{-1} for the ruthenium and osmium trimer anions, respectively. An observed

(37) All calculations were carried out on PDP 8A and 11/34 computers using the Enraf-Nonius CAD 4-SDP programs. This crystallographic computing package is described in: Frenz, B. A. In "Computing in Crystallography"; Schenk, H.; Olthof-Hazekamp, R., van Koningsveld, H., Bassi, G. C., Eds.; Delft University Press: Delft, Holland, 1978; pp 64-71. See also: "CAD 4 and SDP User's Manual"; Enraf-Nonius: Delft, Holland, 1978.

(38) The intensity data were processed as described: "CAD 4 and SDP User's Manual"; Enraf-Nonius: Delft, Holland, 1978. The net intensity $I = (K/NPI)(C - 2B)$, where $K = 20.1166 \times$ (attenuator factor). NPI = ratio of fastest possible scan rate to scan rate for the measurement, $C =$ total count, and $B =$ total background count. The standard deviation in the net intensity is given by $\sigma^2(I) = (K/NPI)^2[C + 4B + (pI)^2]$, where p is a factor used to downweight intense reflections. The observed structure factor amplitude F_o is given by $F_o = (I/Lp)^{1/2}$, where $Lp =$ Lorentz and polarization factors. The $\sigma(I)$'s were converted to the estimated errors in the relative structure factors $\sigma(F_o)$ by $\sigma(F_o) = 1/2(\sigma(I)/I)F_o$.

(39) The function minimized was $\sum w(|F_o| - |F_c|)^2$, where $w = 1/\sigma^2(F_o)$. The unweighted and weighted residuals are defined as $R = (\sum |F_o| - |F_c|)/\sum |F_o|$ and $R_w = [(\sum w(|F_o| - |F_c|)^2)/(\sum w|F_o|)^2]^{1/2}$. The error in an observation of unit weight is $[\sum w(|F_o| - |F_c|)^2/(\text{NO} - \text{NV})]^{1/2}$, where NO and NV are the number of observations and variables, respectively.

(40) Cromer, D. T.; Waber, J. T. "International Tables for X-ray Crystallography"; Kynoch Press: Birmingham, England, 1974; Vol. IV, Table 2.2A. Cromer, D. T. *Ibid.*, Table 2.3.1.

(41) Cromer, D. T.; Ibers, J. A. "International Tables for X-ray Crystallography"; Kynoch Press: Birmingham, England, 1974; Vol. IV, Table 2.2C.

Table II. Positional Parameters and Their Estimated Standard Deviations

atom	x	y	z	atom	x	y	z
Mn	0.13795 (5)	0.7009 (1)	0.76295 (6)	C31	0.1107 (2)	0.9551 (6)	0.1711 (3)
P1	0.10122 (6)	0.7168 (2)	0.33826 (8)	C32	0.1636 (3)	1.0260 (7)	0.1531 (3)
P2	0.10525 (6)	0.7605 (2)	0.17033 (8)	C33	0.1677 (3)	1.1760 (7)	0.1576 (4)
O1	0.0415 (3)	0.6371 (7)	0.6393 (4)	C34	0.1204 (3)	1.2557 (8)	0.1812 (4)
O2	0.1860 (2)	0.4236 (7)	0.8237 (4)	C35	0.0690 (3)	1.1871 (8)	0.2013 (4)
O3	0.2321 (2)	0.8692 (7)	0.7025 (3)	C36	0.0632 (3)	1.0373 (7)	0.1960 (3)
O4	0.0854 (2)	0.8724 (7)	0.8789 (3)	C41	0.0283 (2)	0.7999 (6)	0.3479 (3)
N5	0.1123 (2)	0.6845 (5)	0.2520 (2)	C42	-0.0232 (3)	0.7300 (8)	0.3130 (4)
X1	0.0799 (7)	0.661 (2)	0.6894 (9)	C43	-0.0816 (3)	0.7949 (9)	0.3133 (4)
X2	0.1670 (6)	0.535 (2)	0.8002 (9)	C44	-0.0851 (4)	0.9263 (10)	0.3490 (4)
X3	0.1945 (6)	0.799 (2)	0.7265 (7)	C45	-0.0364 (4)	0.9953 (10)	0.3834 (4)
X4	0.1059 (6)	0.801 (2)	0.8322 (8)	C46	0.0229 (3)	0.9326 (8)	0.3826 (4)
C11	0.0336 (2)	0.7154 (6)	0.1161 (3)	C51	0.1611 (3)	0.8268 (6)	0.3875 (3)
C12	0.0054 (3)	0.8093 (8)	0.0611 (4)	C52	0.2059 (3)	0.8850 (7)	0.3878 (4)
C13	-0.0500 (3)	0.7701 (9)	0.0181 (4)	C53	0.2534 (3)	0.9687 (8)	0.3861 (4)
C14	-0.0754 (3)	0.6385 (8)	0.0306 (4)	C54	0.2538 (3)	0.9929 (9)	0.4628 (4)
C15	-0.0481 (3)	0.5441 (8)	0.0831 (4)	C55	0.2103 (3)	0.9355 (9)	0.5032 (4)
C16	0.0064 (3)	0.5821 (7)	0.1265 (3)	C56	0.1631 (3)	0.8512 (8)	0.4666 (4)
C21	0.1656 (2)	0.6903 (6)	0.1195 (3)	C61	0.1032 (2)	0.5463 (6)	0.3879 (3)
C22	0.1635 (3)	0.7123 (8)	0.0402 (4)	C62	0.0756 (3)	0.5304 (7)	0.4561 (3)
C23	0.2117 (3)	0.6618 (9)	0.0024 (4)	C63	0.0820 (3)	0.3994 (8)	0.4958 (4)
C24	0.2593 (3)	0.5920 (9)	0.0409 (4)	C64	0.1127 (3)	0.2871 (8)	0.4679 (4)
C25	0.2628 (3)	0.5694 (9)	0.1183 (4)	C65	0.1392 (3)	0.3004 (8)	0.4018 (4)
C26	0.2144 (3)	0.6185 (7)	0.1575 (4)	C66	0.1345 (3)	0.4300 (7)	0.3618 (3)

Table III. Distances and Angles for $[\text{Mn}(\text{CO})_2(\text{NO})_2]^-$

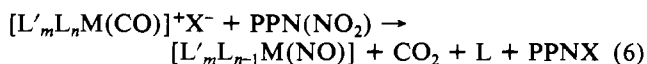
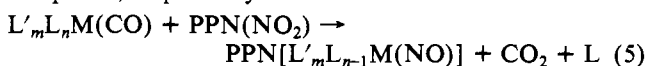
Distances, Å			
Mn-X1	1.745 (6)	X1-O1	1.168 (5)
Mn-X2	1.750 (6)	X2-O2	1.165 (5)
Mn-X3	1.707 (5)	X3-O3	1.163 (5)
Mn-X4	1.730 (6)	X4-O4	1.175 (5)
Angles, deg			
X1-Mn-X2	107.3 (2)	Mn-X1-O1	178.5 (5)
X1-Mn-X3	109.5 (2)	Mn-X2-O2	178.8 (5)
X1-Mn-X4	108.1 (2)	Mn-X3-O3	177.8 (5)
X2-Mn-X3	110.4 (2)	Mn-X4-O4	178.1 (4)
X2-Mn-X4	111.2 (2)	P1-N5-P2	140.2 (2)
X3-Mn-X4	110.3 (2)	(cation)	

isotopic shift of $\nu(^{15}\text{NO})$ to 1451 cm^{-1} for $[\text{Ru}_3(\text{CO})_{10}(^{15}\text{NO})]^-$ supports the assignment of this band. Subtraction of the absorptions due to the PPN^+ cation from the spectrum of $\text{PPN}[\text{Co}(\text{NO})_2(\text{C}-\text{O})_2(\text{NO})]$ resulted in the observation of very weak absorptions at 1323 and 1179 cm^{-1} , which were assigned to the nitro group. An observed isotopic shift of $\nu(^{15}\text{NO}_2)$ to 1300 and 1164 cm^{-1} for $[\text{Co}(\text{NO}_2)_2(\text{CO})_2(\text{NO})]^-$ supports the assignment of these bands.

Kinetic Analysis of the Reaction of $\text{PPN}(\text{NO}_2)$ with $\text{Fe}(\text{CO})_5$ in Acetonitrile. Standard deoxygenated acetonitrile solutions of $\text{PPN}(\text{NO}_2)$ and freshly distilled $\text{Fe}(\text{CO})_5$ were prepared, and at the beginning of the experiment aliquots of each solution were combined in a N_2 -filled Schlenk tube. After immediate mixing, a sample was withdrawn and placed in a nitrogen-flushed NaCl infrared cell, which was quickly placed in the spectrophotometer for continuous monitoring at 1651 cm^{-1} . This procedure required a total of 40 s. The concentration of $[\text{Fe}(\text{CO})_3(\text{NO})]^-$ was determined from a calibration curve of percent transmittance vs. concentration. Duplicate runs of four different concentrations of reactant, followed for at least 2 half-lives, gave excellent agreement with an average $k = 0.111 \pm 0.007\text{ M}^{-1}\text{ s}^{-1}$. In a ninth experiment, no change in rate was observed when a 10-fold excess of triphenylphosphine was added to the solution. In a typical experiment $[\text{Fe}(\text{CO})_5] = [\text{PPN}(\text{NO}_2)] = 0.00729\text{ M}$, and the reaction would be monitored for 40 min. The temperature of the infrared cell was monitored and remained constant at $26 \pm 1^\circ\text{C}$.

Results and Discussion

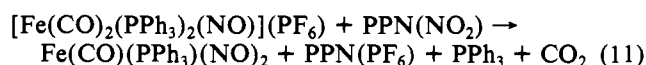
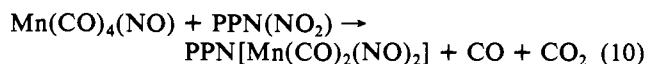
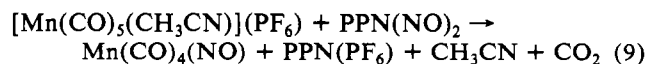
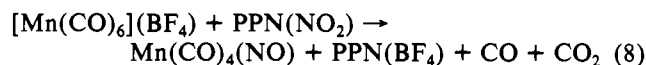
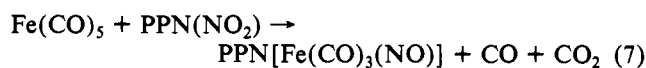
The general reaction of $\text{PPN}(\text{NO}_2)$ with metal carbonyls is summarized in eq 5 and 6 for neutral or cationic starting complexes, respectively.



The ligand labeled L refers to any two-electron donor such as CO or PPh_3 . The net effect of the reaction is to substitute two two-electron donors (CO and L) by a linear nitrosyl (three-electron donor) and a negative charge. These reactions are characterized by a remarkable degree of purity. Monitoring of most of these reactions via infrared spectroscopy shows *only* peaks due to starting material and product.

It is worth mentioning why the PPN cation was chosen for our work. Very simply, $\text{PPN}(\text{NO}_2)$ can easily be prepared in pure crystalline form²⁷ because its solubility in water is less than that of the Cl^- salt and it is not hygroscopic. As mentioned in the Introduction, our goal was to make use of NO_2^- under aprotic conditions. We have experimented with several classic techniques for improving the nucleophilic character of anions, all of which are effective for this reaction. For instance, both NaNO_2 in DMF or Me_2SO and NaNO_2 in THF with a stoichiometric amount of $\text{R}_4\text{N}^+\text{Cl}^-$ (solid-liquid phase-transfer method) work to activate NO_2^- as a nucleophile. $\text{PPN}(\text{NO}_2)$, however, is simpler to use and generates products that are easier to crystallize.

Mononuclear Metal Complexes. Reactions 7-11 summarize the successful use of $\text{PPN}(\text{NO}_2)$ to convert monomeric carbonyl complexes into nitrosyl-containing products.



The reaction of $\text{Fe}(\text{CO})_5$ (eq 7) is conducted at room temperature in THF (although many other solvents can be used). $\text{PPN}(\text{NO}_2)$ is only very slightly soluble in THF, and at the beginning of these reactions the reagent is used as a slurry. Upon addition of 1 equiv of neat $\text{Fe}(\text{CO})_5$, vigorous bubbling occurs and the solution becomes bright yellow. Although most of the reaction is finished within a few minutes, the clear

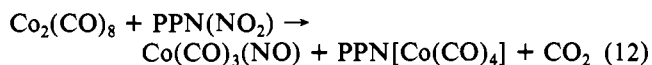
solution is allowed to stir for a total of 30 min. Since there are no side reactions that interfere and the only other products are gases, the solution can be placed directly on a rotary evaporator. The transfer can be conducted in air with no significant effect on the yield. As the solvent is removed, bright yellow crystals of $\text{PPN}[\text{Fe}(\text{CO})_3(\text{NO})]$ form. This material can be used as is, or it can be recrystallized from CH_2Cl_2 /diethyl ether to give an overall yield of 87%. The total time required for the synthesis is less than 1 h, compared to approximately 2 days for the previous method.²³

The reaction of $[\text{Mn}(\text{CO})_6]^+$ with $\text{PPN}(\text{NO}_2)$ (eq 8) in acetonitrile is instantaneous even at $\sim -40^\circ\text{C}$. The product, $\text{Mn}(\text{CO})_4(\text{NO})$, is formed, but due to the difficulty in separating it from the solvent, a direct yield was never obtained. Indirectly we know that it is at least 70% because we have used $\text{Mn}(\text{CO})_4(\text{NO})$ in subsequent reactions in which the overall yield was determined. The related cation $[\text{Mn}(\text{CO})_5(\text{CH}_3\text{CN})]^+$ yields the same nitrosyl product (eq 9). Since this cation can be readily synthesized³⁰ in a one-pot reaction from $\text{Mn}_2(\text{CO})_{10}$, and since it is much easier to handle than $[\text{Mn}(\text{CO})_6]^+$, $[\text{Mn}(\text{CO})_5(\text{CH}_3\text{CN})]^+$ is clearly the preferred starting material to synthesize $\text{Mn}(\text{CO})_4(\text{NO})$.

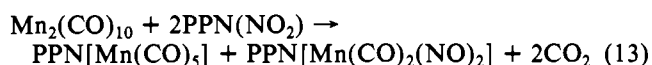
In the presence of additional $\text{PPN}(\text{NO}_2)$, $\text{Mn}(\text{CO})_4(\text{NO})$ is converted into the new nitrosylcarbonylmetalate $[\text{Mn}(\text{C}-\text{O})_2(\text{NO})_2]^-$. Although this can be prepared in high yield in one pot from $[\text{Mn}(\text{CO})_5(\text{CH}_3\text{CN})]^+$, it was impossible to separate the desired product from $\text{PPN}(\text{PF}_6)$. This complication was easily bypassed by starting with only 1 equiv of $\text{PPN}(\text{NO}_2)$. After the first reaction is complete, both the solvent and the $\text{Mn}(\text{CO})_4(\text{NO})$ were distilled under vacuum into a second flask containing the second equivalent of $\text{PPN}(\text{NO}_2)$. This allowed us to obtain an overall 72% yield of analytically pure $\text{PPN}[\text{Mn}(\text{CO})_2(\text{NO})_2]$.

The sterically crowded cation $[\text{Fe}(\text{CO})_2(\text{PPh}_3)_2(\text{NO})]^+$ reacts more slowly with $\text{PPN}(\text{NO}_2)$ relative to the manganese cations. After 30 min in acetonitrile, the infrared spectrum revealed that the only product was $\text{Fe}(\text{CO})(\text{PPh}_3)(\text{NO})_2$. If this solution was allowed to stand, further reaction of $\text{Fe}(\text{CO})(\text{PPh}_3)(\text{NO})_2$ with PPh_3 would occur to produce the known $\text{Fe}(\text{PPh}_3)_2(\text{NO})_2$.³⁵ Chromatography was necessary to purify the product, $\text{Fe}(\text{CO})(\text{PPh}_3)(\text{NO})_2$, which was ultimately recovered in 50% yield.

Dinuclear Metal Complexes. Dicobalt octacarbonyl reacts with 1 equiv of $\text{PPN}(\text{NO}_2)$ in THF within minutes to cleanly form $\text{PPN}[\text{Co}(\text{CO})_4]$ and $\text{Co}(\text{CO})_3(\text{NO})$ (eq 12). The re-

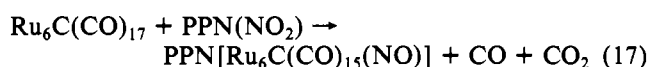
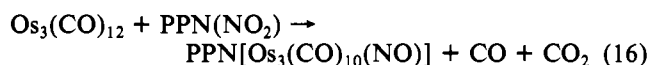
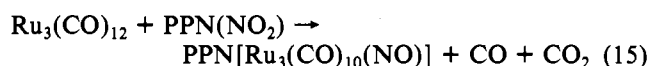
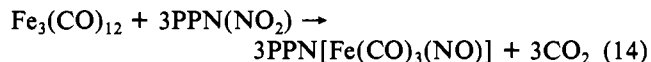


action of manganese is similar (eq 13), except that 2 equiv

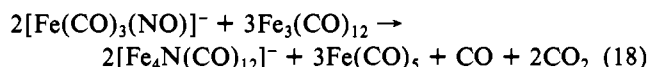


is required for the reaction to go to completion. In analogy to the $\text{Co}_2(\text{CO})_8$ reaction, the anticipated nitrosyl-containing product would be $\text{Mn}(\text{CO})_4(\text{NO})$. Once formed, this apparently must react much faster with $\text{PPN}(\text{NO}_2)$ to form $[\text{Mn}(\text{CO})_2(\text{NO})_2]^-$ (eq 10). No bands due to $\text{Mn}(\text{CO})_4(\text{NO})$ can be observed in the infrared spectrum at any time during the reaction. This reaction is of no value in synthesizing any of the products because they are inseparable. In the cobalt reaction, however, separation of the products can be easily achieved by codistillation of $\text{Co}(\text{CO})_3(\text{NO})$ and solvent into another vessel. In both of these reactions, the adjacent metal fragment is acting as the leaving group L.

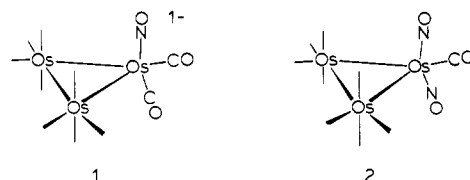
Metal Carbonyl Clusters. Equations 14–17 show the re-



actions of several clusters of the iron triad with $\text{PPN}(\text{NO}_2)$. These reactions are conducted in THF at room temperature, under which conditions they are complete within minutes. The iron trimer does not produce a clean product because of the known reaction¹⁹ of $[\text{Fe}(\text{CO})_3(\text{NO})]^-$ with $\text{Fe}_3(\text{CO})_{12}$ (eq 18).



Both $[\text{Ru}_3(\text{CO})_{10}(\text{NO})]^-$ and $[\text{Os}_3(\text{CO})_{10}(\text{NO})]^-$ are new nitrosyl carbonyl clusters that have structures containing a bridging NO. The complete characterization of these is discussed below. Monitoring the Ru reaction by infrared spectroscopy shows only bands due to starting material and products. When the reaction of $\text{Os}_3(\text{CO})_{12}$ is monitored, clear evidence of an intermediate is observed. Although most of the carbonyl absorbances of the intermediate overlap with those of the product, the peaks at 2085, 2033, 1975, 1876, and 1618 cm^{-1} can be ascribed to this intermediate. The last peak is assigned to a terminal linear nitrosyl bound to a negatively charged osmium atom. This intermediate appears rapidly upon mixing the starting materials and completely converts to the final product after 30 min. Structure 1, which is similar to



that of the known compound $\text{Os}_3(\text{CO})_9(\text{NO})_2$,⁴² (2), is the most reasonable possibility for this intermediate. It is interesting to consider that the rearrangement from Structure 1 to the more stable form with the NO bridging lies along a similar path as that involved in many CO-scrambling mechanisms for carbonyl clusters. $\text{Os}_3(\text{CO})_{12}$ has the highest barrier ($\Delta G_{360}^\ddagger \approx 16.6\text{ kcal/mol}$) for CO scrambling within this triad.⁴³ If we roughly estimate the half-life of this intermediate to be 3–5 min, the ΔG_{298}^\ddagger would equal approximately 21 kcal/mol.

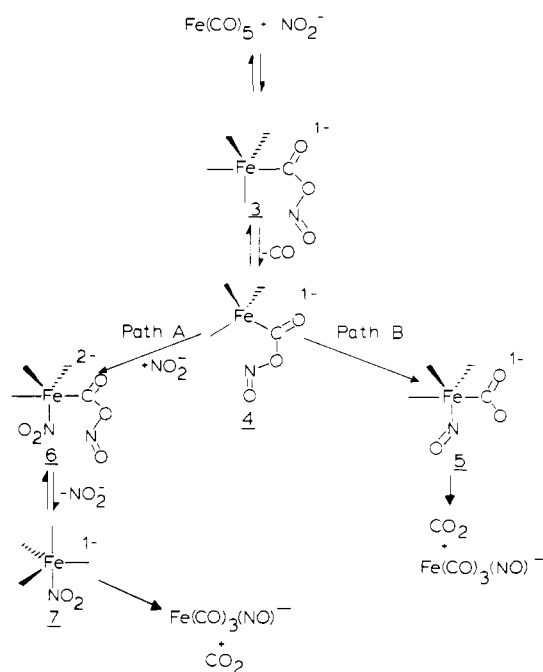
The hexaruthenium carbido cluster reacts rapidly with 1 equiv of $\text{PPN}(\text{NO}_2)$, generating the new carbido cluster $\text{PPN}[\text{Ru}_6\text{C}(\text{CO})_{15}(\text{NO})]$ in high yield. Unlike the case of all previous examples, if excess $\text{PPN}(\text{NO}_2)$ is added further reaction occurs. Apparently, the larger clusters effectively delocalize the negative charge, allowing additional attack by nucleophiles. The full characterization of the product of the second reaction, as well as the reactions of other anionic high-nuclearity clusters with $\text{PPN}(\text{NO}_2)$, is being studied and will be published separately.

Mechanism of $\text{PPN}(\text{NO}_2)$ Reactions. There are several conceivable mechanisms that could be responsible for this reaction. In the following discussion we will concentrate on the reaction of $\text{Fe}(\text{CO})_5$ with $\text{PPN}(\text{NO}_2)$ but suggest that the

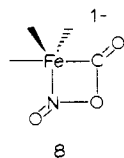
(42) Bhaduri, S.; Johnson, B. F. G.; Lewis, J.; Watson, D. J.; Zuccaro, C. *J. Chem. Soc., Dalton Trans.* **1979**, 557.

(43) Aime, S.; Gambino, O.; Milone, L.; Sappa, E.; Rosenberg, E. *Inorg. Chim. Acta* **1975**, *15*, 53.

Scheme I



results will hold for the other reactants. The kinetic analysis showed the rate-determining step to be first order in both reagents, thus eliminating the possibility of a simple dissociative substitution of NO_2^- for CO, forming the intermediate $[\text{Fe}(\text{CO})_4(\text{NO}_2)]^-$. Nucleophilic attack of NO_2^- on a coordinated carbon monoxide, as shown in Scheme I, is the most reasonable rate-determining step. This is entirely analogous to the reaction of $\text{Fe}(\text{CO})_5$ ⁴⁴ (and many other metal carbonyls⁴⁵) with OH^- or OCH_3^- . Only recently, the rates for the reaction of these two nucleophiles were reported to be 70 and $1.5 \text{ M}^{-1} \text{ s}^{-1}$, respectively.⁴⁴ These studies were conducted in methanol for OCH_3^- and in 70% CH_3OH –30% H_2O for OH^- . The reaction of $\text{PPN}(\text{NO}_2)$ with $\text{Fe}(\text{CO})_5$ in acetonitrile has a second-order rate constant of $0.111 \pm 0.007 \text{ M}^{-1} \text{ s}^{-1}$. The lower reactivity of nitrite relative to OH^- and OCH_3^- with $\text{Fe}(\text{CO})_5$ parallels the differences observed in the reaction of these anions with carbonyl carbons.⁴⁶ The simplest path for conversion of 3 (Scheme I) to the product involves loss of CO to create 4, which is unsaturated, followed by a migratory deinsertion of the NO ligand from CO_2 (path B). The intermediate 4 could be stabilized by chelation of the acyl nitrite ligand as shown in 8. An identical intermediate has been proposed to account



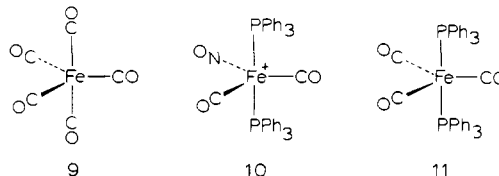
for the reduction of coordinated NO_2 by CO in $\text{Ni}(\text{NO}_2)_2(\text{L})_2$ where $\text{L}_2 = (\text{PEt}_3)_2$ ⁴⁷ and 1,2-bis(diphenylphosphino)ethane.⁴⁸ Collapse of 8 to give 5 could occur simply by N–O bond cleavage. Alternatively, path A involves an anion-catalyzed substitution similar to that first elucidated by Morris and Basolo for the effect of anions on the phosphine substitution of $\text{Fe}(\text{CO})_2(\text{NO})_2$ and $\text{Co}(\text{CO})_3(\text{NO})$.⁴⁹ In an attempt to discriminate between these paths, we reacted nitrite with

$\text{Fe}(\text{CO})_5$ in the presence of a 10-fold excess of PPh_3 . Not only were no phosphine-containing products observed, but the rate of the reaction was identical with those of runs with no added phosphine. Surely, if a second equivalent of nitrite was required to react with 4 (an anion–anion reaction), neutral PPh_3 would compete with this process.

An electron-transfer mechanism would seem very unlikely as the rate-determining step on the basis of the reduction potential for $\text{Fe}(\text{CO})_5$, which is -2.48 V ,⁵⁰ and the oxidation potential for NO_2^- of -0.88 V .⁵¹ A radical process involving an adventitious initiator also seems unlikely since no induction period was observed and reproducible kinetics were obtained with little difficulty.

The first two steps in Scheme I allow us to rationalize the observed selectivity for the loss of a particular ligand without having to differentiate between the two mechanisms. In 3 the negative charge on the metal has increased. Given a choice, the weakest π -accepting ligand on the metal will be lost. This comparison holds well for all of the mono- and dinuclear complexes. In eq 9, CH_3CN is clearly expelled in preference to CO. With $[\text{Fe}(\text{CO})_2(\text{PPh}_3)_2(\text{NO})]^+$ only PPh_3 is eliminated, and in the case of the dimeric metal carbonyls the M–M bond is heterolytically cleaved. Although this rationale also holds for $\text{Fe}_3(\text{CO})_{12}$, the more robust Ru and Os trimers lose CO instead.

Unsuccessful Reactions. Unfortunately, $\text{PPN}(\text{NO}_2)$ does not react with all metal carbonyls in the same manner. It is worth reviewing some of these cases to delineate the scope of the reaction. The simplest cases to understand are those molecules for which the proposed rate-determining step (nucleophilic attack on CO) is too slow. The following series of compounds is particularly illustrative of this point:



Both 9 and 10 react with $\text{PPN}(\text{NO}_2)$ to give the anticipated products within minutes at room temperature. With $\text{Fe}(\text{CO})_3(\text{PPh}_3)_2$, too much electron density is delocalized onto the CO ligands, which greatly reduces their susceptibility to nucleophilic attack.

There are also several other compounds that do rapidly react with $\text{PPN}(\text{NO}_2)$ under mild conditions but, for some reason, have different product-determining steps. The simplest and best characterized example is the reaction of $\text{Co}(\text{CO})_3(\text{NO})$ with $\text{PPN}(\text{NO}_2)$ (eq 19), in which case simple substitution

$$\text{Co}(\text{CO})_3(\text{NO}) + \text{PPN}(\text{NO}_2) \rightarrow \text{PPN}[\text{Co}(\text{NO}_2)(\text{CO})_2(\text{NO})] + \text{CO} \quad (19)$$

occurs. Had this reaction proceeded according to eq 5, the product would be the tricoordinate species $[\text{Co}(\text{CO})(\text{NO})_2]^-$, which would undoubtedly be highly reactive. It may be that the reaction of four-coordinate complexes to give three-coordinate anionic products is thermodynamically unfavorable despite the formation of CO_2 .

The most puzzling reaction studied involved $[\text{Re}(\text{CO})_6]^+$ and $\text{PPN}(\text{NO}_2)$. In acetonitrile, an instantaneous reaction occurs even at low temperatures. In analogy to the manganese system, $\text{Re}(\text{CO})_4(\text{NO})$ was the anticipated product, but it was not observed. The final rhenium-containing product remains unidentified because it is not stable in solution, and we have

(44) Pearson, R. G.; Mauermann, H. *J. Am. Chem. Soc.* **1982**, *104*, 500.(45) Gross, D. C.; Ford, P. C. *Inorg. Chem.* **1982**, *21*, 1702.(46) Edward, J. O.; Pearson, R. G. *J. Am. Chem. Soc.* **1962**, *84*, 16.(47) Doughty, D. T.; Gordon, G.; Stewart, R. P., Jr. *J. Am. Chem. Soc.* **1979**, *101*, 2645.(48) Feltham, R. D.; Kriege, J. C. *J. Am. Chem. Soc.* **1979**, *101*, 5064.(49) Morris, D. E.; Basolo, F. *J. Am. Chem. Soc.* **1968**, *90*, 2536.(50) Pickett, C. J.; Pletcher, D. *J. Chem. Soc., Dalton Trans.* **1975**, 879.

(51) Jones, K. "Comprehensive Inorganic Chemistry"; Bailar, J. C., Jr., Ed.; Pergamon Press: Oxford, 1973; Vol. 2, p 167.

(52) Deleted in revision.

Table IV. Spectroscopic Features of Nitrosyl Carbonyl Complexes

compd	color	$\nu(\text{CO})^a$, cm^{-1}	$\nu(\text{NO})^a$, cm^{-1}	$\delta(^{15}\text{N})^b$
$[\text{Mn}(\text{CO})_2(\text{NO})_2]^-$	red-orange	1964 s, 1881 vs	1646 s, 1609 vs	
$[\text{Fe}(\text{CO})_3(\text{NO})]^-^c$	yellow	1982 m, 1876 s	1650 m	
$[\text{Ru}_3(\text{CO})_{10}(\text{NO})]^-$	deep yellow	2069 w, 2010 s, 2001 vs, 1971 s, 1945 m	$\nu(^{15}\text{NO})$ 1615 1479 (CHCl_3)	398.0 ^e
$\text{HRu}_3(\text{CO})_{10}(\text{NO})^d$	red	2111 w, 2070 vs, 2062 s, 2033 vs, 2019 s, 2001 m (hexane)	$\nu(^{15}\text{NO})$ 1451 (CHCl_3) 1550 m (hexane)	814.4 807.7 ^e
$[\text{Os}_3(\text{CO})_{10}(\text{NO})]^-$	deep yellow	2073 w, 2014 s, 2006 vs, 1987 s, 1940 m	1462 (CHCl_3)	759.8
$[\text{Ru}_6\text{C}(\text{CO})_{15}(\text{NO})]^-$	red	2066 m, 2019 vs, 2002 s, 1960 w, 1836 m, 1811 w	1733 m $\nu(^{15}\text{NO})$ 1698	410.7
$[\text{Co}(\text{NO})_2(\text{CO})_2(\text{NO})]^-$	orange	2022 m, 1950 vs	1717 s	

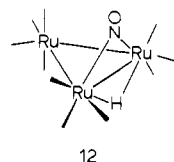
^a All spectra were obtained in THF unless otherwise indicated. ^b All spectra were obtained in CH_2Cl_2 and are reported relative to NH_3 . ^c Reference 58. ^d Reference 36. ^e This work.

not been able to crystallize it. In acetonitrile it exhibits only two carbonyl absorbances at 2045 s and 1995 m cm^{-1} , reminiscent of neutral $\text{Re}(\text{CO})_5\text{X}$ molecules.⁵³ The surprising result of this reaction was found by monitoring the gas evolved after addition of the $\text{PPN}(\text{NO}_2)$. Both CO_2 and N_2O were present while no CO was detected. It is not unreasonable that the species initially formed is $\text{Re}(\text{CO})_5\text{NO}$, which would have a bent M-N-O geometry. Dimerization of this through the NO to give a hyponitrite group may be responsible for the N-N bond formation.⁵⁴

Characterization of the New Compounds. The reaction of $\text{PPN}(\text{NO}_2)$ with $\text{Mn}(\text{CO})_4(\text{NO})$ generates the nitrosyl-carbonylmetalate $\text{PPN}[\text{Mn}(\text{CO})_2(\text{NO})_2]$. This is only the second example of an anionic complex containing only NO and CO as ligands. It can be recrystallized from THF/ether, giving air-sensitive red-orange crystals. The infrared spectrum is just that expected for a species having C_{2v} symmetry and is very similar to $\text{Fe}(\text{CO})_2(\text{NO})_2$ except for the shift to lower energy due to the negative charge. As shown in Table IV, the $\nu(\text{CO})$ and $\nu(\text{NO})$ absorbances appear very close to those of $\text{PPN}[\text{Fe}(\text{CO})_3(\text{NO})]$. A single-crystal X-ray crystallographic study was undertaken to compare with the structures of related carbonyl nitrosyl complexes. Although the overall structure can be assigned, the location of the carbon and nitrogen atoms could not be confidently established and we are forced to treat the CO and NO ligands as a 50/50 mixture. The Mn-X bond distances (Table III) are shorter than both the M-N and M-C distances of the neutral tetrahedral complexes $\text{Fe}(\text{CO})_2(\text{NO})_2$ ($\text{Fe}-\text{C} = 1.84$ (2) Å, $\text{Fe}-\text{N} = 1.77$ (2) Å) and $\text{Co}(\text{CO})_3(\text{NO})$ ($\text{Co}-\text{C} = 1.83$ (2) Å, $\text{Co}-\text{N} = 1.76$ (3) Å),⁵⁵ despite the fact that Mn is a larger atom. When comparison is made to the Mn-C (1.87 (1) Å) and Mn-N (1.80 (1) Å) bond distances in $\text{Mn}(\text{CO})_4(\text{NO})$,⁵⁶ the difference between a neutral and negatively charged complex is accentuated. This decrease in the Mn-X distances is a result of increased π -delocalization of electron density from the metal to the ligands. It is interesting that all of the Mn-X distances are shorter than the average Fe-C distance of 1.76 (2) Å in the dianion $[\text{Na}(\text{crypt})]_2[\text{Fe}(\text{CO})_4]$.⁵⁷ This is a result of the averaging of the C and N to metal bond distances.

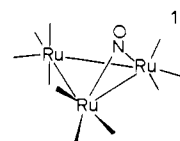
The new clusters $[\text{Ru}_3(\text{CO})_{10}(\text{NO})]^-$ and $[\text{Os}_3(\text{CO})_{10}(\text{NO})]^-$ were characterized by elemental analyses, by infrared and ^{15}N NMR spectroscopy, and by their reaction with protons to give the known clusters $\text{HRu}_3(\text{CO})_{10}(\text{NO})$ and $\text{HOs}_3(\text{CO})_{10}(\text{NO})$. These hydrido clusters were previously prepared by Johnson and co-workers³⁶ by the reaction of NO^+ with

$[\text{HM}_3(\text{CO})_{11}]^-$ ($\text{M} = \text{Ru}, \text{Os}$). An X-ray crystallographic analysis of the phosphite-substituted Ru cluster showed that they have the framework of structure 12, which is charac-



12

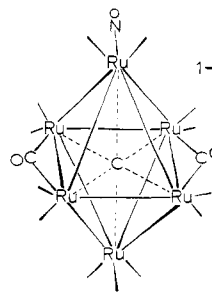
teristic of the $\text{HM}_3(\text{CO})_{10}\text{X}$ formulation. We believe that the structure of the anions is similar to that of their protonated analogues, 13. The infrared spectrum shows no evidence for



13

bridging carbonyls or terminal nitrosyl ligands. We were able to observe the bridging NO stretching frequency in both the Ru and Os anions using subtraction techniques in FT IR spectroscopy. This allowed us to remove the interference due to the solvent and the PPN counterion. The absorbances appear at 1479 and 1462 cm^{-1} for the Ru and Os clusters, respectively. In $\text{HRu}_3(\text{CO})_{10}(\text{NO})$, the bridging NO stretch occurs at 1550 cm^{-1} . This $\sim 80\text{-cm}^{-1}$ drop is anticipated, as it is of similar magnitude as the change in $\nu(\text{CO})$ in going from a neutral to an anionic cluster. In the Ru cluster we also prepared a sample that was 90% enriched with ^{15}NO . The $\nu(\text{NO})$ was lowered by 20 cm^{-1} , which is similar to the 35- cm^{-1} $\Delta\nu(\text{NO})$ for $[\text{Fe}(\text{CO})_3(\text{NO})]^-$.⁵⁸

The structure of $[\text{Ru}_6\text{C}(\text{CO})_{15}(\text{NO})]^-$ cannot be assigned with certainty without an X-ray structural analysis. From the observation of a terminal nitrosyl and two bridging carbonyl absorbances in the infrared spectrum, structure 14 can be suggested.



14

- (53) Braterman, P. S. "Metal Carbonyl Spectra"; Academic Press: London, 1975; p 223.
 (54) Bhaduri, S. A.; Bratt, I.; Johnson, B. F. G.; Khair, A.; Segal, J. A.; Walters, R.; Zuccaro, C. *J. Chem. Soc., Dalton Trans.* 1981, 234.
 (55) Brockway, L. O.; Anderson, J. S. *Trans. Faraday Soc.* 1937, 33, 1233.
 (56) Frenz, B. A.; Enemark, J. H.; Ibers, J. A. *Inorg. Chem.* 1969, 8, 1288.
 (57) Teller, R. G.; Finke, R. G.; Collman, J. P.; Chin, H. B.; Bau, R. *J. Am. Chem. Soc.* 1977, 99, 1104.

- (58) Pannell, K. H.; Chen, Y. S.; Belknap, K. L. *J. Chem. Soc., Chem. Commun.* 1977, 362.

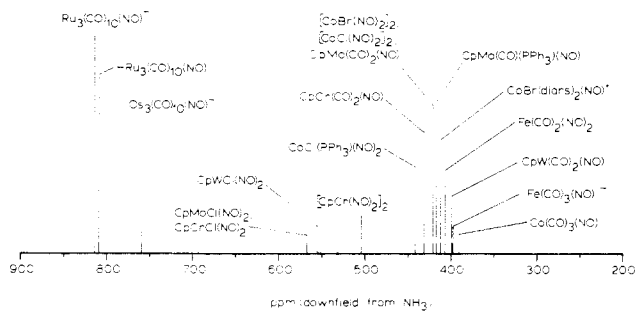


Figure 2. Summary of the nitrogen chemical shifts for several metal nitrosyl complexes. The data for compounds not prepared in this paper are taken from ref 59 and 60.

Nitrogen-15 magnetic resonance spectroscopy of metal nitrosyls has been little studied, and few guidelines exist for the use of this technique. Figure 2 summarizes the nitrogen chemical shifts obtained from ^{15}N as well as ^{14}N measurements^{59,60} (the chemical shifts of the two nuclei are equivalent) of some of the lower valent metal nitrosyls. The measurements made in this study on the three trinuclear clusters are the first reported for complexes having exclusively bridging NO ligands. The nitrogen chemical shift of the NO ligand in the clusters appears far downfield from what can loosely be classified as the terminal NO region. Within the clusters studied, there is a relatively small ($\Delta\delta = 6.7$) upfield shift upon protonation, whereas the change from Ru to Os causes a 54.6 ppm upfield shift in the resonance. Upfield shifts upon descending a periodic group have also been observed in the mononuclear nitrosyl complexes that have been studied.⁵⁹ As far as comparing the $\delta(^{15}\text{N})$ of the clusters with mononuclear compounds having only CO and NO as ligands, there is a 400 ppm downfield shift in going from a terminal to doubly bridging environment.

Simple CO substitution of $\text{Co}(\text{CO})_3(\text{NO})$ has been well documented with a wide variety of nucleophiles.^{61,62} As shown in eq 19, the nitro complex $\text{PPN}[\text{Co}(\text{NO}_2)(\text{CO})(\text{NO})]$ is formed when $\text{PPN}(\text{NO}_2)$ is reacted with $\text{Co}(\text{CO})_3(\text{NO})$. Infrared spectroscopy establishes the similarity between $[\text{Co}(\text{NO}_2)(\text{CO})_2(\text{NO})]^-$ and $[\text{Co}(\text{CN})(\text{CO})_2(\text{NO})]^-$ ⁶³ and can also be valuable for differentiating N-bound from O-bound NO_2 . Weak and broad absorbances at 1323 and 1179 cm^{-1} are assigned to the symmetric and antisymmetric N-O stretches of an N-bound ligand. This is the result expected on the basis of related d^{10} complexes such as $\text{Ni}(\text{NO}_2)(\text{PMe}_3)_2(\text{NO})$.⁶⁴

(59) Botto, R. E.; Kolthammer, B. W. S.; Legzdins, P.; Roberts, J. D. *Inorg. Chem.* **1979**, *18*, 2049.

(60) Becker, W.; Beck, W. Z. *Naturforsch., B: Anorg. Chem., Org. Chem.* **1970**, *25B*, 101.

(61) Thorsteinson, E. M.; Basolo, F. J. *Am. Chem. Soc.* **1966**, *88*, 3929.

(62) Nast, R.; Rohmer, M. Z. *Anorg. Allg. Chem.* **1956**, *285*, 271.

(63) Behrens, H.; Lindner, E.; Schindler, H. *Chem. Ber.* **1966**, *99*, 2399.

Summary

The use of $\text{PPN}(\text{NO}_2)$ to convert metal carbonyls into nitrosyl carbonyl complexes has resulted in the high-yield preparations of several mono- and polynuclear compounds. The overall reaction involves replacement of two carbonyls with a nitrosyl and a negative charge. When the starting mononuclear carbonyl complex contains two-electron-donor ligands other than CO, such as PPh_3 or CH_3CN , one of these is selectively dissociated in place of one of the carbonyls. In simple dinuclear species, the metal-metal bond is selectively cleaved, initially generating two different monomers: the carbonylmethylate and the neutral nitrosyl carbonyl product. One of the most valuable applications of $\text{PPN}(\text{NO}_2)$ involves the conversion of carbonyl clusters into nitrosyl carbonyl clusters. Many neutral carbonyl clusters are already known to be susceptible to nucleophilic attack by species such as hydroxide, and we anticipate they will also react with $\text{PPN}(\text{NO}_2)$. Preliminary results suggest that with clusters containing greater than five or six metals the charge resulting from the first attack of nitrite is effectively delocalized, allowing subsequent reaction. With $\text{Fe}(\text{CO})_5$ in acetonitrile, the second-order kinetics support a mechanism involving nucleophilic attack of nitrite on coordinated carbon monoxide as the rate-determining step. Continued exploration of the reactions of $\text{PPN}(\text{NO}_2)$ is in progress.

Acknowledgment. We gratefully acknowledge the National Science Foundation for support of this work (Grant No. CHE 8106096), Timothy Yanta for experimental assistance, and Bill Brenamen and Rudd Meiklejohn of the 3M Co. for assistance in obtaining the FT IR spectra. R.E.S. wishes to thank the University of Minnesota for an Institute of Technology Corporate Associate Fellowship (1980-1982).

Note Added in Proof. An independent report of the synthesis of $\text{PPN}[\text{Ru}_6\text{C}(\text{CO})_{15}(\text{NO})]$ has appeared (Johnson, B. F. G.; Lewis, J.; Nelson, W. J. H.; Puga, J.; Raithby, P. R.; Braga, D.; McPartlin, M.; Clegg, W. *J. Organomet. Chem.* **1983**, *243*, C13).

Registry No. **9**, 13463-40-6; **10**⁺ PF_6^- , 21374-47-0; **12**, 73230-19-0; **13**⁻ PPN^+ , 79085-63-5; **14**⁻ PPN^+ , 85849-59-8; $\text{PPN}[\text{Fe}(\text{CO})_3(\text{NO})]$, 61003-17-6; $[\text{Mn}(\text{CO})_5(\text{CH}_3\text{CN})]\text{PF}_6$, 37504-44-2; $\text{PPN}[\text{Mn}(\text{C}_2\text{O}_2)(\text{NO})_2]$, 79061-79-3; $\text{Fe}(\text{CO})(\text{PPh}_3)(\text{NO})_2$, 14591-53-8; $\text{Co}(\text{C}_2\text{O}_2)(\text{NO})$, 14096-82-3; $\text{PPN}[\text{Co}(\text{NO}_2)(\text{CO})_2(\text{NO})]$, 85803-23-2; $\text{Co}_2(\text{CO})_8$, 10210-68-1; $\text{Mn}_2(\text{CO})_{10}$, 10170-69-1; $\text{Ru}_3(\text{CO})_{12}$, 15243-33-1; $\text{Os}_3(\text{CO})_{12}$, 15696-40-9; $\text{PPN}[\text{Os}_3(\text{CO})_{10}(\text{NO})]$, 79061-77-1; $\text{HO}_3(\text{CO})_{10}(\text{NO})$, 73238-03-6; $\text{Ru}_6\text{C}(\text{CO})_{17}$, 27475-39-4; $[\text{Mn}(\text{CO})_6](\text{BF}_4)$, 15557-71-8; $\text{Fe}_3(\text{CO})_{12}$, 17685-52-8; $\text{PPN}(\text{NO}_2)$, 65300-05-2.

Supplementary Material Available: Tables of observed and calculated structure factors, positional and thermal parameters, and general temperature factor expressions (19 pages). Ordering information is given on any current masthead page.

(64) Krieger-Simonsen, J.; Elblaze, G.; Dartiguenave, M.; Feltham, R. D.; Dartiguenave, Y. *Inorg. Chem.* **1982**, *21*, 230.